

A Flexible BIST Strategy for SDR Transmitters

Emanuel Dogaru^{*†}, Filipe Vinci dos Santos^{*} and William Rebernak[†]

^{*}Thales Chair on Advanced Analog Design, SUPELEC

Gif-sur-Yvette, France

Email: filipe.vinci@supelec.fr

[†]THALES Communications & Security

Gennevilliers, France

Abstract—Software-defined radio (SDR) development aims for increased speed and flexibility. The advent of these system-level requirements on the physical layer (PHY) access hardware is leading to more complex architectures, which together with higher levels of integration pose a challenging problem for product testing. For radio units that must be field-upgradeable without specialized equipment, Built-in Self-Test (BIST) schemes are arguably the only way to ensure continued compliance to specifications. In this paper we introduce a loopback RF BIST technique that uses Periodically Nonuniform Sampling (PNS2) of the transmitter (TX) output to evaluate compliance to spectral mask specifications. No significant hardware costs are incurred due to the re-use of available RX resources (I/Q ADCs, DSP, GPP, etc.). Simulation results of an homodyne TX demonstrate that Adjacent Channel Power Ratio (ACPR) can be accurately estimated. Future work will consist in validating our loopback RF BIST architecture on an in-house SDR testbed.

Keywords—BIST, In-Field Test, Periodically Nonuniform Sampling, Software Radios, Mixed-Signal/RF Test, Subsampling, Spectral Mask Estimation

I. INTRODUCTION

Software-Defined Radio (SDR) development aims for increased speed and flexibility [1]. Multi-mode wideband SDRs attempt to overcome harsh conditions and spectrum scarcity by dynamic sensing and adaptation to the environment [2]. The advent of these system-level requirements on the physical layer (PHY) access hardware is leading to more complex receiver (RX) and transmitter (TX) architectures, which together with higher levels of integration pose a challenging problem for product testing.

Established mixed-signal and RF test strategy [3], [4] are either too time-consuming (thus costly) or cannot guarantee compliance with multiple modulation standards, including those yet to appear. Thus, the flexibility and the complexity of SDR platforms make these systems hard to test. Moreover, for radio units that must be field-upgradeable without specialized equipment, Built-in Self-Test (BIST) schemes are arguably the only way to ensure continued compliance to specifications.

The loopback approach is undoubtedly one of the most promising RF BIST technique for RF transceivers [5]–[8]. Nonetheless, it suffers from one major drawback: fault-masking. Fault masking arises because RX and TX faults are not observable separately. Test stimuli and observation sites must be then carefully chosen to minimize fault-masking conditions (sensitization techniques).

Several sensitization techniques that aim to improve loopback observability have been proposed. In [7], [9] the authors

rely on analytical behavioral models and simple input stimuli (sinusoid or multi-tone signals) to extract the most important nonlinearities and IQ imbalances in a quadrature transceiver (phase mismatch, gain mismatch, DC offset, and time-skew). This approach yields few test-escapes and demands low computational effort. However, it is limited by the completeness of the model. Under configurations unforeseen by the model, the entire test strategy will fail.

Another interesting RF BIST strategy is “alternate test”, in which the standard specifications are predicted from a set of “easily” measurable parameters that are strongly correlated with the specifications one wishes to check [10]–[13]. The alternate tests are based on heuristic models, obtained a priori through simulations. These alternate tests are prone to errors such as test-escapes and yield loss [14], which are hard to predict. Test metrics estimation techniques can help only if an extremely large number of units can be measured beforehand. Tactical radio unit production runs are far below these numbers.

From the point of view of SDR platforms, a common shortcoming of the previous mentioned RF BIST proposals is that they are tied to specific operating modes (frequency, modulation, standard, etc.) and architectures, and cannot be applied easily to multi-mode tactical radio units. Test strategies that use a given fault model must necessarily hold assumptions on the operation modes of the radio, whereas in SDR platforms nearly all aspects are field-configurable. In this scenario, specification-based testing seems unavoidable. The outstanding challenge for SDR testing is then how to conduct specification testing without external equipment.

A BIST strategy that attempts to meet this challenge was introduced in [15], [16]. In order to improve the loopback observability, the authors proposed to first characterize the TX using a subsampling architecture based on Periodically Nonuniform Sampling of second order (PNS2). However, as presented, the approach required external (off-unit, off-radio, off-board or off-chip, according to the level of integration) computing capability (still, at reduced cost w.r.t. a full ATE).

In this paper we improve the work presented in [15], [16] and introduce a practical standalone implementation for the proposed BIST technique based on digital filters. Our proposed solution is scalable across a wide set of complex specifications and can be easily applied for in-field testing with small additional hardware requirements. Compared to existing analog/RF test techniques, this approach is not limited to a given TX architecture and does not rely on an ad-hoc TX model, which makes it ideal for SDR testing.

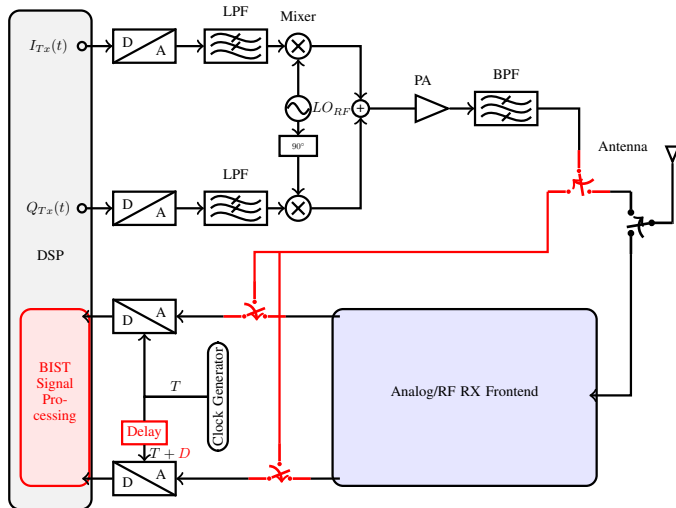


Fig. 1. Architecture of an homodyne TX. The red blocks are the modifications required by the RF BIST technique. In this technique, similarly to the loopback approach, the signal of interest is routed back to the DSP and further analyzed. The key difference is that the RX in this case is bypassed and instead a BIST circuitry is employed.

A crucial specification for TX compliance is the Adjacent Channel Power Ratio (ACPR), which is rarely addressed by existing BIST techniques [11] due to the complexity of the measurement. Our proposed BIST scheme aims to fill this gap and extract the ACPR accurately. It can also handle less demanding measurements, such as IP3, gain, and I/Q imbalance without any hardware modifications, using existing signal processing algorithms.

To confirm our expectations, we built a behavioral model of an homodyne transmitter and ran extensive simulations in *Matlab*. The simulations demonstrate that ACPR can be effectively and accurately obtained by our BIST architecture across the whole operating band.

The main contribution of this work consists in proposing a BIST strategy based on periodical nonuniform bandpass sampling that targets the spectral mask estimation at the output of the TX for any mode of operation and architecture. Compared to earlier works, in this paper we introduce a practical implementation that can be wholly implemented within the SDR platform.

The remainder of this paper is organized as follows. Section II gives an overall description of the BIST system we propose. The key ideas and important limitations are analyzed. Afterwards, in Section III we discuss a candidate architecture that implements the proposed strategy. Section IV shows the results obtained in simulation. Finally, our conclusions and future developments are given in Section V.

II. GENERAL DESCRIPTION

In this section we give a general description of the proposed RF BIST architecture.

The block diagram of the modified transceiver is shown in Fig. 1. Our objective is to monitor the modulated signal at the output stage. To do that, one must route it back to the processing unit (DSP, GPP). The I/Q ADCs can be used for this, as in a

classical loopback test. The rest of the RX is bypassed, to avoid fault-masking, and the output signal is translated to baseband for A/D conversion by subsampling. Subsampling is widely used both for analog BIST and spectrum sensing. However it introduces limitations w.r.t. the sampling rate and frequency bands to be translated. These limitations can be relaxed by using both ADCs as a single one (i.e. raising sampling rate by time interleaving) and using periodical nonuniform sampling of second order (PNS2).

It is assumed that the output waveform of the TX is shaped by a bandpass filter that is functional, i.e. the RF signal is limited to a roughly defined frequency range. This assumption is realistic, and does not impose any new constraints on the TX architecture.

The TX test strategy can be separated in two steps:

- 1) PNS2 sampling. In this step the samples required by the PNS2 technique are acquired. The PNS2 sampling process and its limitations are discussed in [15].
- 2) Signal reconstruction using PNS2. This step can be carried out either externally by some auxiliary equipments or on-board, as shown in Section III. We have determined that reconstruction is feasible using only two FIR filters with complex coefficients, making it worthwhile to pursue an on-board (standalone) implementation. Further details on how to derive the filters coefficients and on the associated computational effort are presented in Section III.

To sum up, the key advantages of the proposed strategy are:

- flexibility over a wide range of operating modes. In fact, the PNS2-based BIST is able to characterize the TX across all frequency bands simply by updating the coefficients of two digital filters.
- minimum of extra hardware requirements. In the best case, only a digitally controlled delay element and two FIR filters are needed.
- removes fault-masking prior to loopback test of RX.
- non-intrusive during normal radio operation.

However, some inherent limitations will affect our proposed architecture. It is well known that the phase noise of the sampling clock degrades the performance of the bandpass sampling technique. Nonetheless, in [17] it is shown that the clock jitter requirement for a bandpass sampling receiver are similar to the requirements for the local oscillator (LO) in a mixing receiver. In addition, the analog input bandwidth of the existing S/H stages of the two ADCs must cover all the RF signals we want to monitor. If that's not the case, two suitable S/H circuits must be added.

Finally, the proposed architecture can also be used for other purposes, such as during the calibration step for digital pre-distortion techniques that improve the TX linearity.

III. PROPOSED ARCHITECTURE

In this section we discuss a practical implementation of the test strategy described in the previous section. First, some theoretical results regarding the periodically nonuniform sampling

are introduced. Afterwards, it's shown how the reconstruction of nonuniformly sampled bandlimited signals can be carried out by two discrete-time finite impulse response (FIR) filters. Several approaches for computing the filter tap coefficients are reviewed. Our choice is to discretize a continuous-time formula. Other ways to obtain values for the filter tap coefficients are also considered and discussed.

A. Periodically Nonuniform Bandpass Sampling (PNS2)

It is well known that a continuous time signal $f(t)$ with Fourier transform $F(\nu)$, limited to a non-zero frequency range $|\nu| < B$ can be reconstructed from its samples $f(nT/2)$, where $T = 1/B$. This technique is commonly called Nyquist sampling. It has also been demonstrated in [18], [19] that if $F(\nu)$ is limited to a frequency range $f_l < |\nu| < f_l + B$ (see Fig. 2a), then $f(t)$ can also be reconstructed from a set of uniformly spaced samples $f(nT/2)$, as long as the ratio f_l/B is a positive ratio integer. This sampling scheme is called Periodically Bandpass Sampling of First Order (PBS) or Uniform Bandpass Sampling. If the previous requirements of signal band locations are not met, Kohlenberg [19] showed that $f(t)$ can still be reconstructed from two sets of uniform samples $f(nT)$ and $f(nT + D)$. This sampling scheme is called Periodically Nonuniform Bandpass Sampling of Second Order (PNS2), and it will be described in detail further on. The advantages of using PNS2 over PBS in this context are given in [15], [16]. From the point of view of SDR testing, the key advantage is greater flexibility than traditional subsampling.

PNS2 relies on two sets of uniformly spaced samples as depicted graphically in Fig. 2. Fig. 2a represents the original passband signal to be reconstructed. Fig 2b sketches the spectrum $F_A(\nu)$ resulting from sampling by the sample set A . For improved clarity, the top figure shows only the positive frequency components $F_{A+}(\nu)$ resulting from sampling, while the bottom figure depicts only the negative frequency components $F_{A-}(\nu)$. Similarly, the spectra of the set B is depicted as $F_{B+}(\nu)$ and $F_{B-}(\nu)$ in Fig. 2c. Finally, $S_A(\nu)$ and $S_B(\nu)$ from Fig. 2d represent the interpolants (reconstructing filters) which are designed to restore the original signal. They are computed in such a way that the negative frequency components are suppressed in the band of interest. A detailed analysis on how these interpolants are computed is given in [20].

One should note that our purpose is not to reconstruct the signal at the original RF position but to shift it to baseband, or as close as possible to it. The repetitive nature of the spectra $F_A(\nu)$ and $F_B(\nu)$ (see Fig. 2) offers the possibility of recovering not only the original function but a frequency-translated version of it. Therefore, the red spectrum in Fig. 2 represents the interpolants that reconstruct the original signal at baseband. Let us denote this original baseband-shifted signal by $f_{bb}(t)$.

The following relations can be derived:

$$\begin{aligned} f_{bb}(t) &= s_A(t) * f_A(t) + s_B(t) * f_B(t) \\ &= \sum_{n=-\infty}^{+\infty} [f(nT)s_A(t - nT) + f(nT + D)s_B(t - nT - D)] \end{aligned} \quad (1)$$

where D is the phase delay between the sets of samples and the two interpolants, $s_A(t)$ and $s_B(t)$ are defined by their

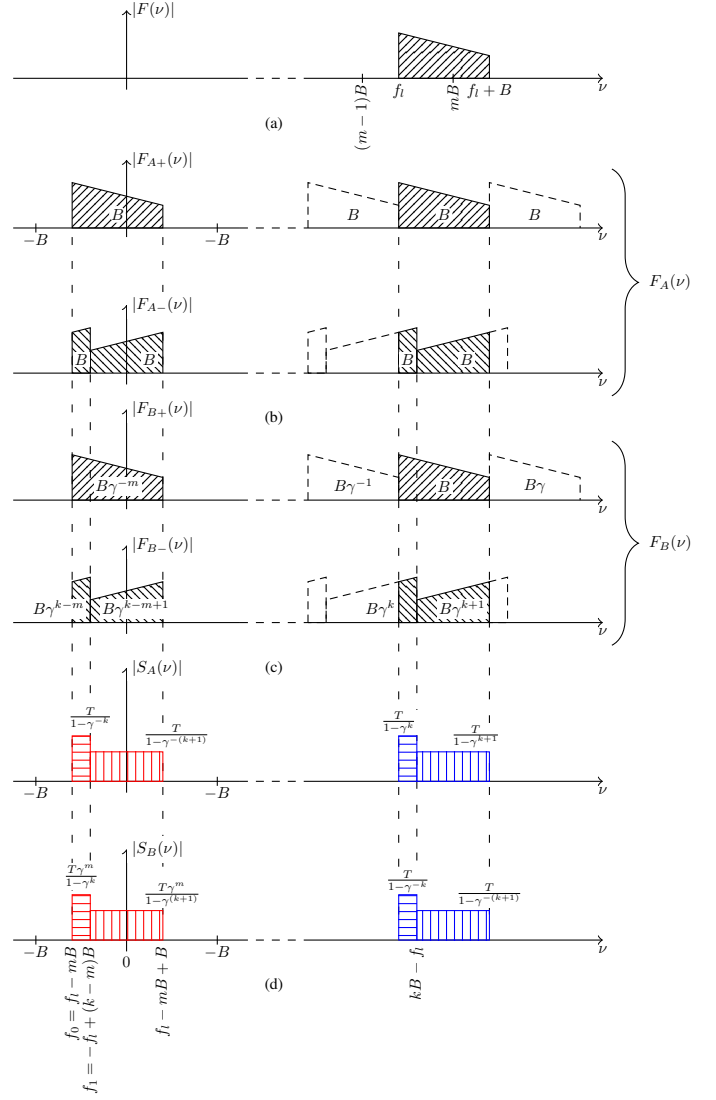


Fig. 2. Periodically nonuniform bandpass sampling of second order. Fig. 2a represents the original passband signal to be reconstructed. Fig 2b sketches the spectrum $F_A(\nu)$ resulting from sampling by the sample set A . The top figure shows only the positive frequency components $F_{A+}(\nu)$ resulting from sampling, while the bottom figure shows only the negative frequency components $F_{A-}(\nu)$. The spectra of the set B is depicted as $F_{B+}(\nu)$ and $F_{B-}(\nu)$ in Fig. 2c. $S_A(\nu)$ and $S_B(\nu)$ in Fig. 2d represent the interpolants (reconstructing filters) which are designed to restore the original signal.

frequency response:

$$S_A(\nu) = \begin{cases} \frac{T}{1-\gamma^{-k}} & \text{if } f_0 < \nu < f_1 \\ \frac{T}{1-\gamma^{-(k+1)}} & \text{if } f_1 < \nu < f_0 + B \\ 0 & \text{otherwise} \end{cases} \quad (2a)$$

$$S_B(\nu) = \begin{cases} \frac{T\gamma^m}{1-\gamma^k} & \text{if } f_0 < \nu < f_1 \\ \frac{T\gamma^m}{1-\gamma^{(k+1)}} & \text{if } f_1 < \nu < f_0 + B \\ 0 & \text{otherwise} \end{cases} \quad (2b)$$

$$k = \lceil 2f_l/B \rceil, m = \lceil f_l/B \rceil, \gamma = e^{-j2\pi BD} \quad (2c)$$

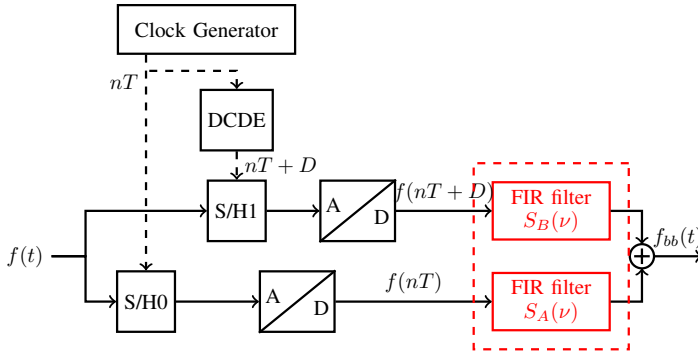


Fig. 3. Complete block diagram of the proposed BIST architecture

Using (2a), $s_A(t)$ is obtained as:

$$s_A(t) = \int_{f_0}^{f_0+B} S_A(\nu) e^{j2\pi\nu t} d\nu \quad (3)$$

or after several manipulations:

$$s_A(t) = \frac{e^{-j\pi BDk} (e^{j2\pi f_1 t} - e^{j2\pi f_0 t})}{2\pi Bt \sin \pi BDk} + \frac{e^{-j\pi BDk^+} (e^{j2\pi(f_0+B)t} - e^{j2\pi f_1 t})}{2\pi Bt \sin \pi BDk^+} \quad (4)$$

Similarly, for $s_B(t)$ one obtains:

$$s_B(t) = -s_A(t) e^{-j2\pi BD(k-m)} \quad (5)$$

The relation (2) is valid provided that D meets the following constraints:

$$D \neq nT/k \quad (6a)$$

$$D \neq nT/(k+1), \forall n \in \mathbb{N} \quad (6b)$$

From (4) and (5), as well from Fig. 2d, one can readily observe that the interpolating functions required to shift the original signal to baseband are complex. On the other hand, the filters that recover the signal at the carrier frequency have real coefficients. In the next section we will show how the theoretical results given here can be mapped to a digital filter implementation.

B. Digital Implementation of PNS2

As shown in the previous section, PNS2 allows the reconstruction and the frequency-shifting of a bandpass signal from two sets of periodic nonuniformly spaced samples. In this section we discuss the digital implementation requirements of this technique. The block diagram of the entire BIST circuitry is presented in Fig. 3. For the sake of completeness, the left side of the figure shows the circuitry added to acquire the necessary samples for the reconstruction. This circuit was introduced and analyzed in [16]. Our concern here is how to design the highlighted digital filters that can reconstruct the bandpass signal at baseband. There are several approaches possible. Due to space limitations we'll develop here only one and at the end of the section we'll succinctly discuss other options.

Our approach is based on implementing the equations (2), (4) and (5) using FIR filters with complex coefficients.

The time-continuous interpolants could be implemented at the theoretical minimum sampling rate (on average) of $2B$. Unfortunately, in the general case, the discretization of these interpolants cannot be done at the minimum sampling-rate without causing aliasing. In fact, it can be readily observed from the geometrical representation in Fig. 2d that the signal of interest occupy a band of B Hz, and lies somewhere between $-B$ and B , depending on the original signal position. Therefore, to preclude aliasing, the baseband signal must be oversampled by a minimum factor of two. Considering this and the relations (4) and (5), the FIR filters can be expressed as:

$$f_{bb}(t) = \sum_{n=-n_w/2}^{n_w/2} f(t - nT/2) s_A^n + f(t - nT/2 - D) s_B^n \quad (7a)$$

$$s_A^n = s_A(t) \Big|_{t=nT/2} \quad (7b)$$

$$s_B^n = s_B(t) \Big|_{t=nT/2+D} \quad (7c)$$

The FIR taps in (7) were obtained by truncating the continuous-time interpolants (4) and (5). In this context, truncating means choosing a finite number ($n_w + 1$) of coefficients. In order to minimize the effects of truncation, a window functions is employed (in our work we chose a rectangular Kaiser window, for simplicity). In [21] it's shown that, if a raised cosine filter is used as a window function, the reconstruction filters lead to a more robust estimation w.r.t. noise and uncertainty.

Alternatively, one could adopt a conceptually different approach, as proposed in [22]. There, the reconstruction issue is posed as a filter bank design problem. The filters coefficients are analytically obtained using least-squares formulation. One of the advantages of this alternate approach would be that it allows one to choose the level of approximation error with respect to the length of the filter by the mean of the optimization criterion. However, we did not pursue this later method because our filter coefficients were good enough with our simpler method.

C. Discussions

Even if the theoretical minimum sample rate for PNS2 is $2B$, we have shown that for a practical digital implementation the original signal must be oversampled by a factor of two. Interestingly, digital implementations using minimum-rate sampling are possible in few particular cases: when the signal is integer positioned ($f_l = nB + B/2, n \in \mathbb{N}$) or half-integer positioned ($f_l = nB, n \in \mathbb{N}$). These cases are treated in [20]. In these situations, the practical implementation is simplified and the cost is reduced. Depending on the level of flexibility required by the test technique and on the available digital resources, one could choose either to implement the general PNS2-based BIST strategy presented in Section III-B or to go with the simplified version.

Finally, examining Fig. 2, one can observe that the baseband-shifted signal is not centered around DC (0 Hz), but around $f_l - mB + B/2$. A digital frequency-shifting could be considered but, as our final objective is the spectral mask estimation, this feature isn't warranted and it's not discussed further.

IV. SIMULATION RESULTS

In order to validate the theoretical framework described in this paper, the behavioral model of an homodyne transmitter was constructed. Our choice was guided by the flexibility, high level of integrability and good performance of the homodyne transmitter. The block diagram of our homodyne transmitter is depicted in the top of the Fig. 1.

The periodically nonuniform technique, on which the entire framework is based, would require an explicit simulation of each carrier cycle. To keep the computational effort reasonable, the simulations presented in this paper are based on behavioral passband models [23]. The simulations were carried out in Matlab.

The TX BIST architecture shown in Fig. 3 was realized with two 10-bits ADCs, each one sampling at a rate of 100 MSamples/s. We consider that there are no gain or offset mismatches between the two ADCs, since those can be corrected by a previous ADC calibration step. The clock generator that drives the sample-and-hold circuit is affected by a gaussian distributed time-skew jitter of 3 ps rms. The phase delay $D = 90$ ps between the two ADCs is estimated separately by the LMS-based technique described in [15]. Each filter has $n_w + 1 = 61$ taps, that were obtained using the first procedure described in Section III-B.

The targeted waveform is an one code-channel W-CDMA signal used in third generation communication devices and described by the 3GPP @TS 125.104 standard [24]. It occupies a 5 MHz band at $f_c = 1890$ MHz. The signal was generated using Communications System Toolbox/Matlab.

Fig. 4 shows the power spectrum of the estimated signal (red) compared to the original signal (blue). For convenience and comparison purposes, both spectra of interest are plotted relative to the DC. It can be observed that the original signal is estimated accurately by the proposed technique. However, the result of thermal noise aliasing that occurs due to the sampling operation is visible. The aliasing contributes to the degradation of our spectral quality figure of merit.

A. ACPR estimation

The ACPR (Adjacent Channel Power Ratio) is one of the most important system-level figures of merit. It measures the amount of distortion generated by transmitter in the adjacent-frequency channel relative to the power in the main channel. It quantifies the effect of nonlinear distortions and is commonly specified for every digital transmission standard.

The ACPR also gives valuable information for the designer about the influence of nonlinearities in the analog path on the quality of the modulated signal. Together with the modulation scheme, the ACPR sets the maximum allowable nonlinearity of the power amplifier, the last active circuit block before the antenna.

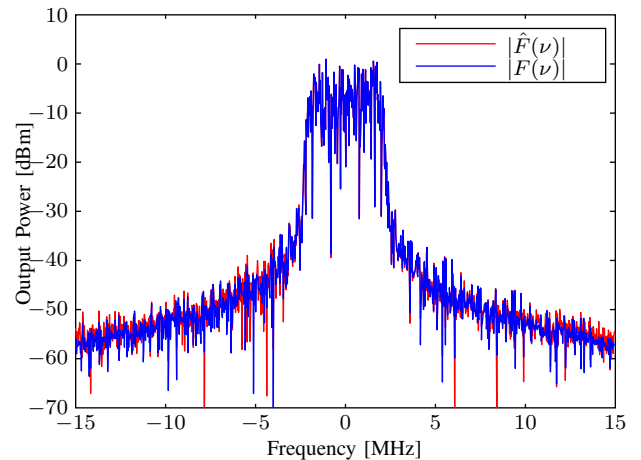


Fig. 4. Output power spectrum. Real spectrum (blue) versus estimated spectrum (red)

ACPR measurement is required by any stringent final product qualification procedure. In a BIST strategy the ACPR measurement is usually replaced by a simpler figure of merit: the third-order interception point (IP3). IP3 is calculated using simple input stimulus (sinusoid or multi-tone signals) and it cannot guarantee the DUT behavior in realistic scenarii, particularly for wide-bandwidth modulation schemes. On the other hand, ACPR measurements are conducted while the DUT is driven by complex digitally modulated waveforms. This characteristic makes the ACPR a realistic and highly desirable measurement for a BIST architecture, and is the target of our efforts.

The W-CDMA standard defines the ACPR as the ratio of the average power in the main channel and any adjacent channels. The main channel has a bandwidth of 3.84 MHz centered around the carrier frequency. W-CDMA requires ACPR measurement for four adjacent channels, located at -10, -5, 5, 10 MHz away from the main channel center frequency. In all cases, the adjacent channel power is obtained using a 3.84-MHz bandwidth.

Using the previous definitions, the ACPR was calculated for different simulation scenarii, using both the original passband signal and the estimated one. The results are listed in Table I. Because of the limited space, only the ACPR@-10MHz and ACPR@5MHz are presented, but the other two ACPR simulations gave similar results. One can observe that the power of the main channel P_{MC} is estimated quite accurately while the power in the adjacent channels are estimated with an accuracy of ± 2 dBc. The W-CDMA standard specifies that ACPR values be below -45 dBc at +/- 5MHz offsets, and below -50 dBc at +/- 10 MHz offsets. We ran simulations in which the TX signal of interest met the specifications (scenario 1) or violated them (scenarii 2 and 3). The proposed BIST technique was able to uncover the specification violation every time.

Finally, if higher accuracy is desired, one could average the frequency spectra over several FFT windows. Such an averaged spectrum is presented in Fig. 5 for scenario 3, where 50 FFT windows have been used. The ACPR estimation results for this case are listed in the last row of Table I. One can clearly see that the estimation accuracy of the PNS2-based technique has improved at both offsets.

TABLE I. ACPR ESTIMATION USING PNS2

Scenario	P_{MC} [dBm]	ACPR@-10MHz [dBc]	ACPR@5MHz [dBc]
	real/estimated	real/estimated	real/estimated
1	10.29 / 10.31	-59.8 / -57	-48.5 / 48.3
2	13.14 / 13.12	-61 / -59	-40.9 / -42
3	16.69 / 16.66	-61 / -59	-42 / -43
av. 50	16.7 / 16.71	-61 / -59.8	-42 / -41.9

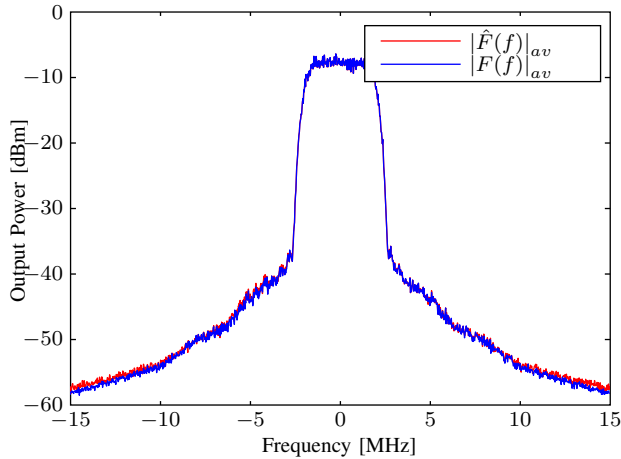


Fig. 5. Output power spectrum averaged over 50 FFT windows. Real spectrum (blue) versus estimated spectrum (red)

V. CONCLUSIONS AND FUTURE WORKS

In this paper we introduce a Built-In Self-Test strategy designed for the test/characterization of the output stage in a multistandard radio. The strategy is based on Periodically Nonuniform Sampling of second order and targets spectral mask estimation at the output of the TX for any mode of operation and architecture. Discussions regarding the advantages of this technique as well as its limitations have been presented. We have also shown that the proposed architecture is amenable to efficient digital implementation. Analytical expressions and simulation results show the feasibility and the potential of the proposed technique.

Future work will consist in experimental validation of the proposed architecture on an in-house SDR testbed. The implementation of a loopback RF BIST technique without fault-masking for standalone test of a complete SDR transceiver seems achievable.

ACKNOWLEDGMENT

This research has been supported by a CIFRE ANRT grant. The Supélec-Thales Chair on Advanced Analog Design acknowledges the financial support of the Thales Group.

REFERENCES

- [1] M. Woh, Y. Lin, S. Seo, S. Mahlke, and T. Mudge, "Analyzing the next generation software defined radio for future architectures," *J. Signal Process. Syst.*, vol. 63, no. 1, pp. 83–94, Apr. 2011. [Online]. Available: <http://dx.doi.org/10.1007/s11265-009-0402-z>
- [2] J. Ma, G. Li, and B.-H. Juang, "Signal processing in cognitive radio," *Proceedings of the IEEE*, vol. 97, no. 5, pp. 805–823, 2009.
- [3] R. Wolf, M. Slamani, J. Ferrario, and J. Bhagat, *Advances in Electronic Testing: Challenges and Methodologies*. Netherlands: Springer, 2006, ch. 10 - RF Testing.

- [4] P. Cruz, N. Carvalho, and K. Remley, "Designing and testing software-defined radios," *IEEE Microw. Mag.*, vol. 11, no. 4, pp. 83–94, 2010.
- [5] M. Negreiros, L. Carro, and A. A. Susin, "Reducing test time using an enhanced RF loopback," *J. Electron. Testing*, vol. 23, no. 6, pp. 613–623, 2007.
- [6] J. Dabrowski and J. Bayon, "Mixed loopback BIST for RF digital transceivers," in *Proc. IEEE Defect and Fault Tolerance in VLSI Systems (DFT 2004)*, Oct. 2004, pp. 220 – 228.
- [7] A. Nassery and S. Ozev, "An analytical technique for characterization of transceiver IQ imbalances in the loop-back mode," in *Design, Automation Test in Europe (DATE)*, 2012, pp. 1084–1089.
- [8] A. Haldes, S. Bhattacharya, G. Srinivasan, and A. Chatterjee, "A system-level alternate test approach for specification test of RF transceivers in loopback mode," in *Proc. Int. Conf. on VLSI Design (VLSID'05)*, 2005, pp. 132–137.
- [9] E. Erdogan and S. Ozev, "Single-measurement diagnostic test method for parametric faults of I/Q modulating RF transceivers," in *VLSI Test Symposium, 2008. VTS 2008. 26th IEEE*, May 2008, pp. 209 –214.
- [10] V. Natarajan, R. Senguttuvan, S. Sen, and A. Chatterjee, "Built-in test enabled diagnosis and tuning of RF transmitter systems," *VLSI Design*, 2008.
- [11] A. Halder, S. Bhattacharya, and A. Chatterjee, "System-level specification testing of wireless transceivers," *IEEE Trans. VLSI Syst.*, vol. 16, no. 3, pp. 263–276, 2008.
- [12] A. Haider, S. Bhattacharya, and A. Chatterjee, "Automatic multitone alternate test-generator for RF circuits using behavioral models," in *International Test Conference, 2003. Proceedings. ITC 2003*, vol. 1, 2003, pp. 665–673.
- [13] D. Maliuk, H.-G. Stratigopoulos, H. Huang, and Y. Makris, "Analog neural network design for RF built-in self-test," in *IEEE International Test Conference (ITC), 2010*, 2010, pp. 1–10.
- [14] N. Kupp, H.-G. Stratigopoulos, P. Drineasz, and Y. Makris, "On Proving the Efficiency of Alternative RF Tests," in *2011 IEEE/ACM International Conference on Computer-Aided Design (ICCAD)*, 2011.
- [15] E. Dogaru, F. Vinci, and W. Rebernak, "LMS-based RF BIST architecture for multistandard transmitters," *Proc. IEEE Defect and Fault Tolerance in VLSI Systems (DFT 2013)*, Oct. 2013.
- [16] —, "An RF BIST architecture for output stages of multistandard radios," *Military Communications and Information Systems Conference (MCC2013)*, May 2013.
- [17] V. Arkesteijn, E. A. M. Klumperink, and B. Nauta, "Jitter requirements of the sampling clock in software radio receivers," *IEEE Trans. Circuits Syst. II*, vol. 53, no. 2, pp. 90–94, 2006.
- [18] Y.-P. Lin and P. Vaidyanathan, "Periodically nonuniform sampling of a new class of bandpass signals," in *Proc. IEEE Digital Signal Processing Workshop*, Sep. 1996, pp. 141 –144.
- [19] A. Kohlenberg, "Exact interpolation of band limited functions," *J. Appl. Physics*, vol. 24, no. 12, pp. 1432 –1436, Dec. 1953.
- [20] D. A. Linden, "A discussion of sampling theorems," *Proceedings of the IRE*, vol. 47, no. 7, pp. 1219–1226, 1959.
- [21] M. Chabert and B. Lacaze, "Fast convergence reconstruction formulas for periodic nonuniform sampling of order 2," in *IEEE Trans. Acoust., Speech, Signal Process.*, 2012, pp. 3793–3796.
- [22] H. Johansson and P. Lowenborg, "Reconstruction of nonuniformly sampled bandlimited signals by means of time-varying discrete-time fir filters," *EURASIP Journal on Advances in Signal Processing*, vol. 2006, no. 1, p. 064185, 2006. [Online]. Available: <http://asp.eurasipjournals.com/content/2006/1/064185>
- [23] J. Chen, "Modeling RF systems," The Designer's Guide Community, 2005. [Online]. Available: <http://www.designers-guide.org/Modeling/modeling-rf-systems.pdf>
- [24] (2013, Jul.) Universal mobile telecommunications system (umts); base station (bs) radio transmission and reception (fdd) (3gpp ts 25.104 version 11.6.0 release 11). [Online]. Available: http://www.etsi.org/deliver/etsi_ts/125100_125199/125104/11.06.00_60/ts_125104v110600p.pdf